Supporting Information (SI)

Facile Synthesis of Highly Efficient One-Dimensional Plasmonic Photocatalysts through Ag@Cu_2O Core−Shell Heteronanowires

Jinyan Xiong,[†] Zhen Li,[*,†,‡] Jun Chen,[§] Shanqing Zhang,[⊥] Lianzhou Wang,[∥] and Shixue Dou[†]

[†]Institute for Superconducting & Electronic Materials and §Intelligent Polymer Research Institute, The University of Wollongong, Wollongong NSW 2500, Australia

[⊥]Centre for Clean Environment and Energy Environmental Futures Centre, Griffith School of Environment, Griffith University, Southport QLD 4222, Australia

[∥]Nanomaterials Centre, School of Chemical Engineering & Australian Institute for Bioengineering and Nanotechnology, The University of Queensland, Brisbane QLD 4072, Australia

[‡]School of Radiation Medicine and Radiation Protection, Soochow University, 199 Ren Ai Road, Suzhou Industrial Park, Suzhou 215123, China

[*]Corresponding author: zhenl@uow.edu.au; Tel: +61-2-42215163; Fax +61-2-42215731.

Figure S1

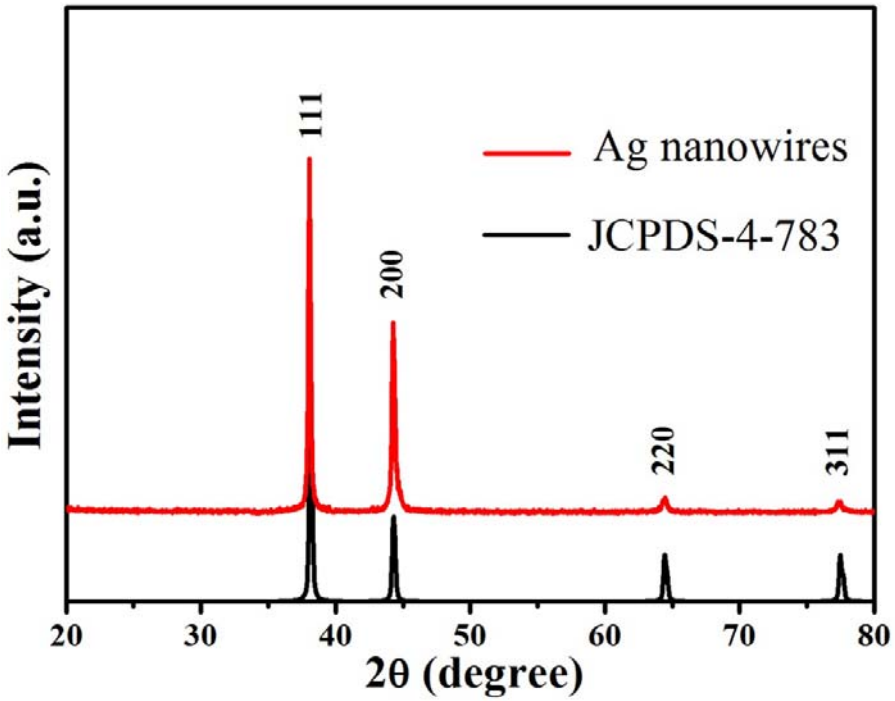

Figure S1. XRD pattern of as-prepared Ag nanowires (Ag NWs).

Figure S2

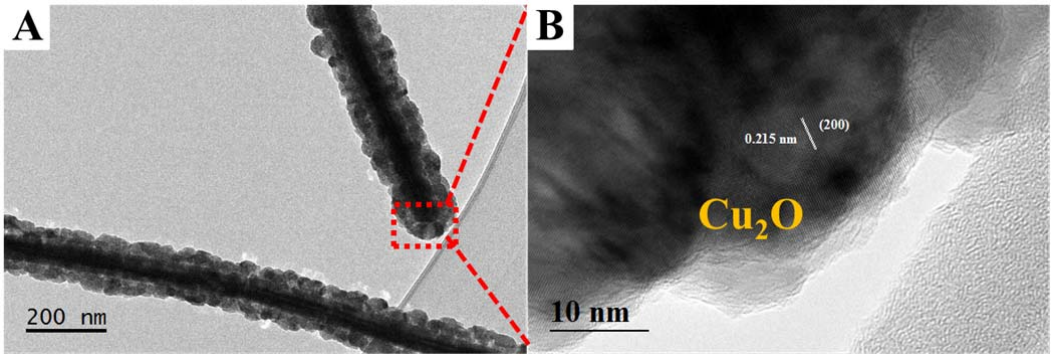

Figure S2. (A)TEM and (B) HRTEM images of the 1D Ag@Cu_2O core-shell heteronanowire.

Figure S3

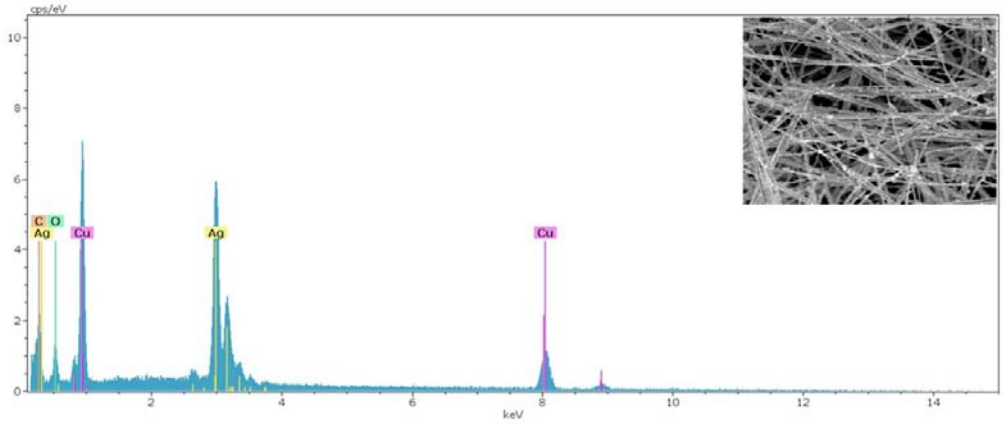

Figure S3. EDS pattern of as-synthesized 1D Ag@Cu_2O core-shell heteronanowires.

Figure S4

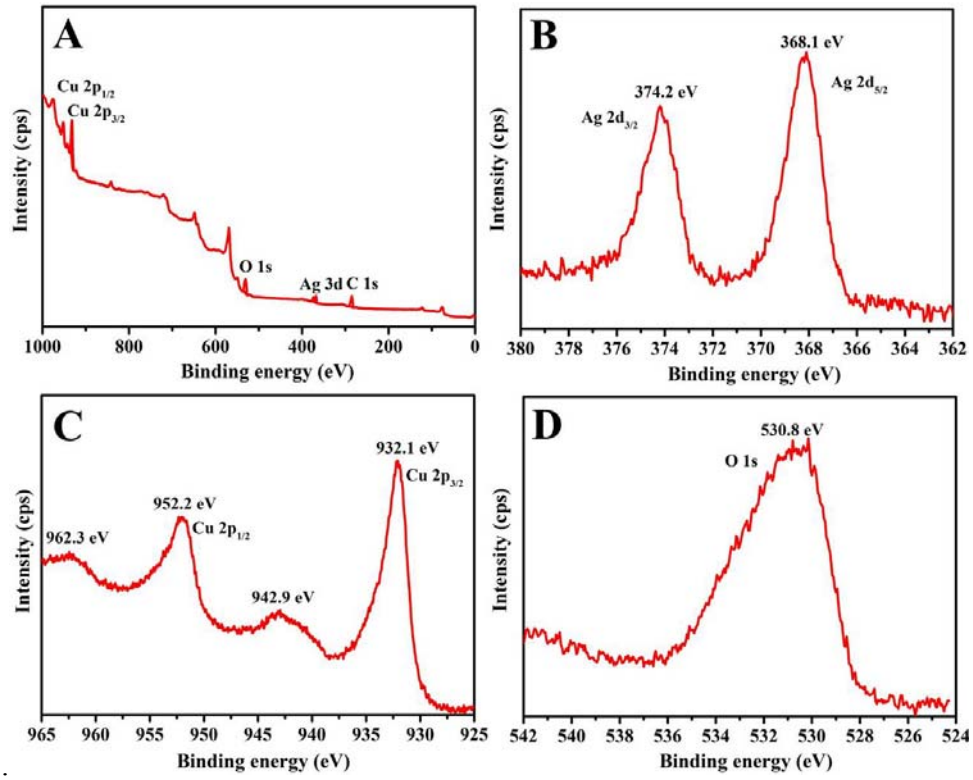

Figure S4. XPS spectra of the 1D Ag@Cu_2O core-shell heteronanowires: (A) survey-scan spectrum, (B) Ag 2d, (C) Cu 2p, and (D) O 1s.

X-ray photoelectron spectroscopy (XPS) measurement has been performed to investigate the surface elemental composition and electronic state of Ag@Cu_2O core-shell heteronanowires, as shown in Figure S4. The survey spectrum in Figure S4(A) shows that except for C, Cu, O and Ag, no other elements are observed in the spectrum, indicating the high purity of the product. The peak at 284.5 eV can be readily assigned to the binding energies of C1s. High-resolution spectra of Ag, Cu and O species are shown in Figure S4(B-D), respectively. Two strong peaks at 374.2 eV and 368.1 eV [Figure S4(B)] are respectively assigned to Ag2d 3/2 and Ag2d 5/2, which correspond to pure metallic Ag according to the reported results.[1, 2] From the high resolution scanning spectra of Cu 2p

[Figure S4(C)], two main peaks at binding energies of 932.1 and 952.2 eV, together with two shakeup satellites at 942.9 and 962.3eV, were observed in the sample. The peaks at 932.1 and 952.2 eV can be attributed to the binding energies of Cu 2p3/2 and Cu 2p1/2 from Cu^{+}.[3-5] The satellite peaks at 942.9 and 962.3 eV located at higher binding energies are typically associated with Cu^{2+} in CuO or probably $Cu(OH)_2$ species,[3, 5, 6] implying the presence of Cu^{2+} on the sample surface. These results demonstrate that copper species in $Ag@Cu_2O$ are mainly present as Cu^{+}, and only a small amount of Cu^{2+} is presented in the sample. This is reasonable as Cu_2O is easy to be oxidized in the process of experiment.[7] Surface Cu_2O could be oxidized into CuO and/or $Cu(OH)_2$ species when they were exposed in air with humidity. The peak at 530.8 eV in Figure S4(D) corresponds to O 1s, which is originated from the lattice oxygen of Cu_2O.[5, 8]

Figure S5

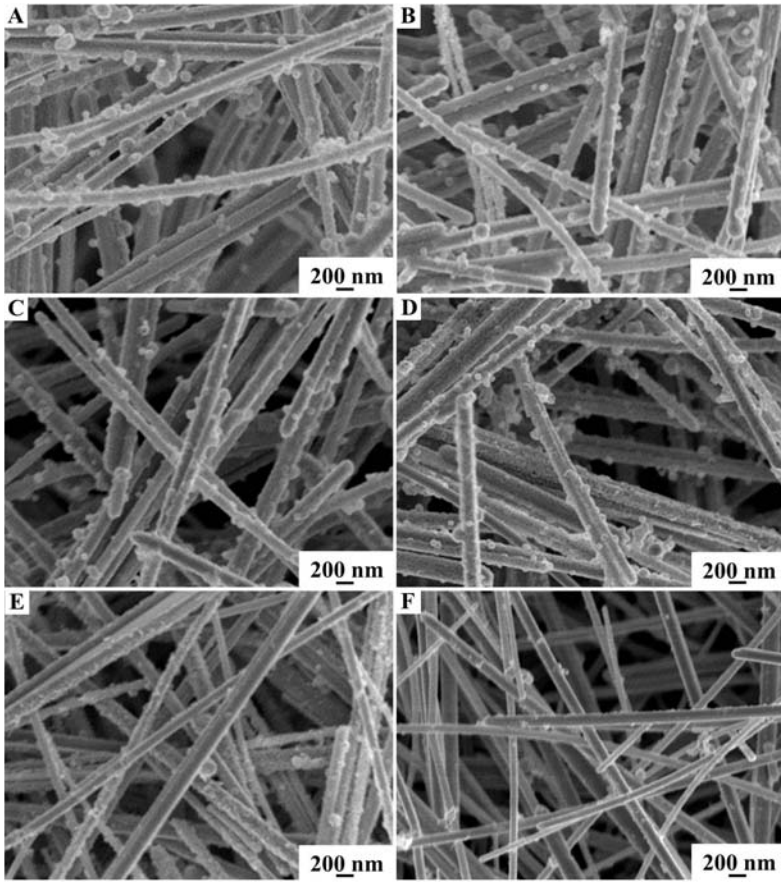

Figure S5. SEM images of the products obtained at different reaction times: (A) 2 min, (B) 20 min, (C) 40 min, (D) 60 min, (E) 12 h and (F) 24 h.

Figure S6

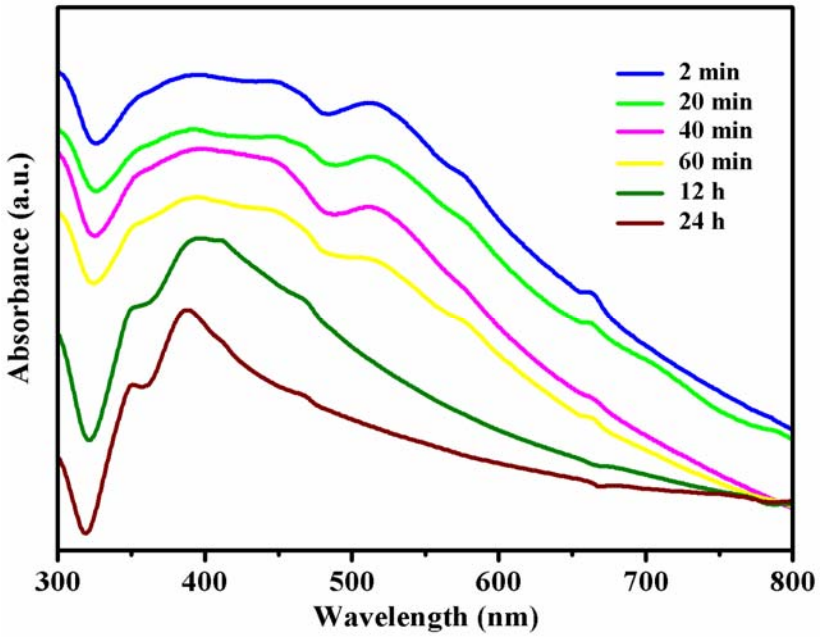

Figure S6. UV-vis absorption spectra of the products obtained at different reaction times.

Figure S7

Figure S7. Photographs of reaction systems composited of Ag NWs, Cu $(NO_3)_2$ solution and N_2H_4 before and after reaction at different stages.

Figure S8

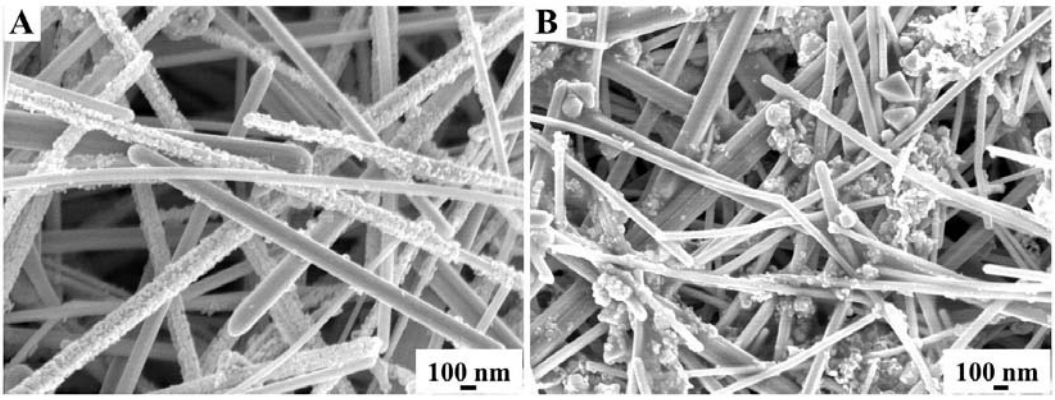

Figure S8. SEM images of the products prepared in the presence of different concentration of Cu^{2+}: (A) 0.1 M and (B) 0.2 M.

Figure S9

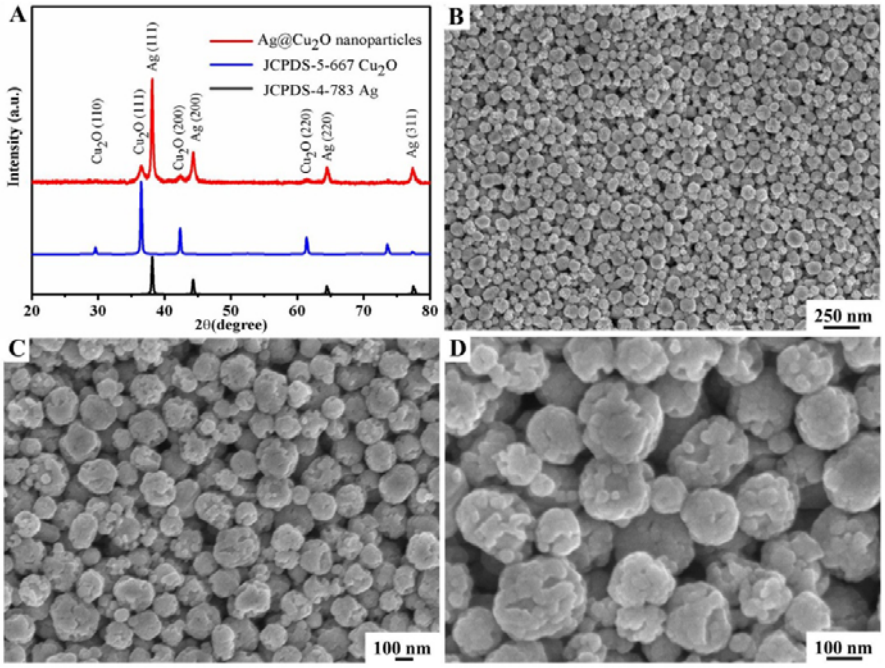

Figure S9. (A) XRD pattern and (B-D) SEM images of the Ag@Cu_2O nanoparticles.

Figure S10

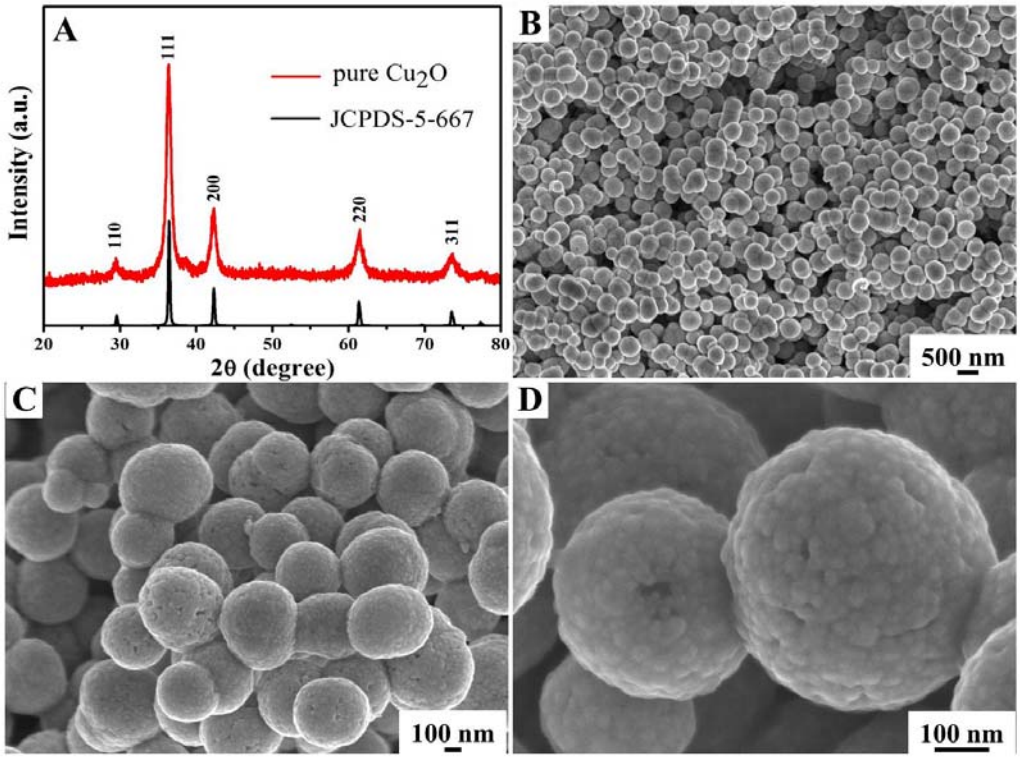

Figure S10. (A) XRD pattern and (B-D) SEM images of the pure Cu_2O.

Figure S11

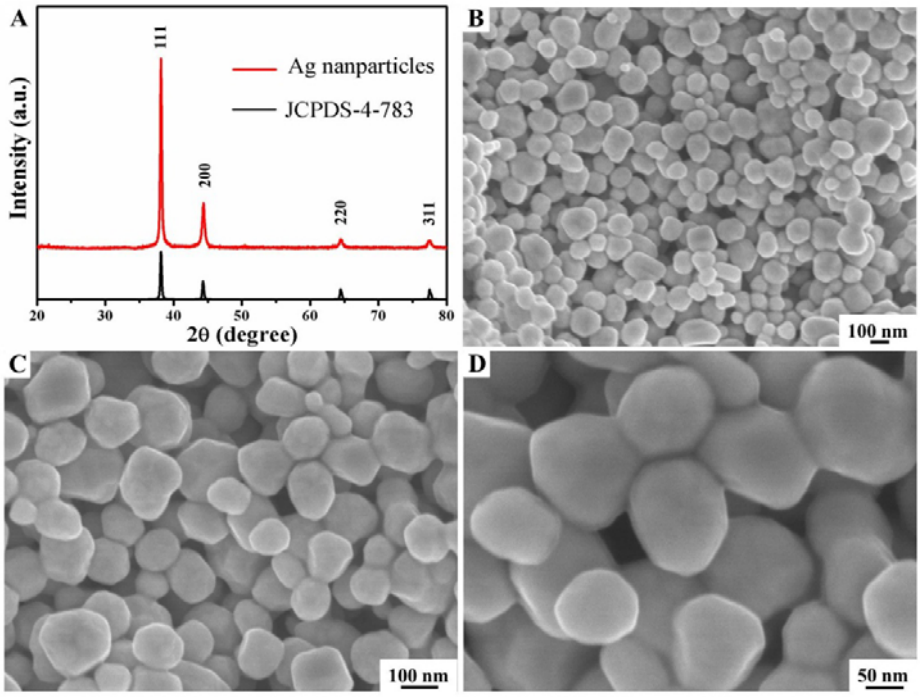

Figure S11. (A) XRD pattern and (B-D) SEM images of the Ag nanoparticles.

Figure S12

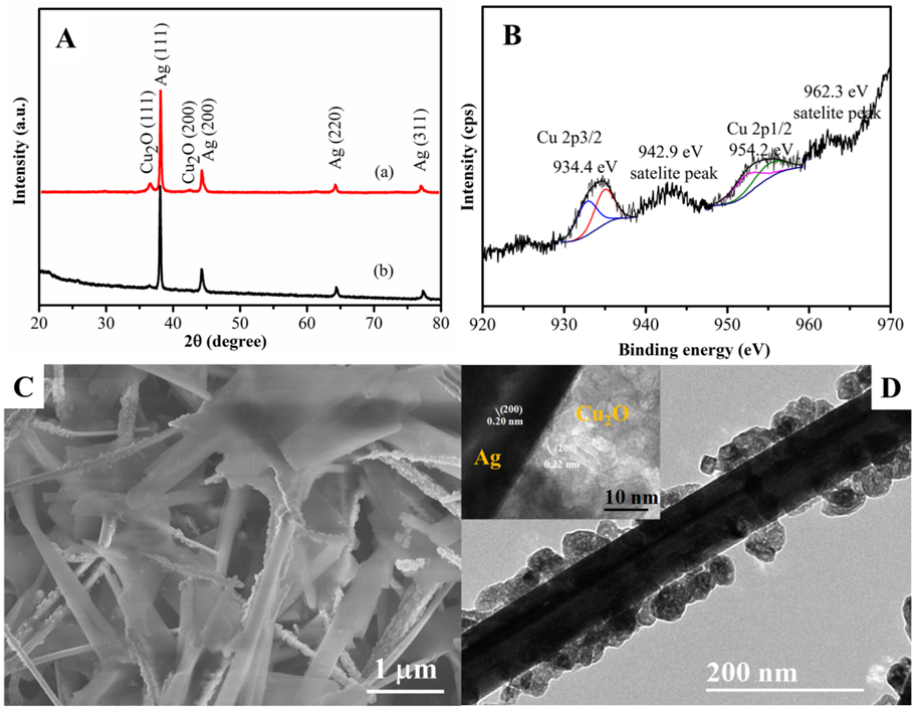

Figure S12. (A) XRD patterns of the sample before (a) and after (b) photocatalytic test; (B) XPS spectrum of Cu 2p, (C) SEM image and (D) TEM image of the sample after photocatalytic test.

References

1. Ji, R.; Sun, W.; Chu, Y., One-Step Hydrothermal Synthesis of Ag/Cu_2O Heterogeneous Nanostructures over Cu Foil and Their SERS Applications. *RSC Adv.* **2014,** *4*, 6055-6059.
2. Wu, W.-T.; Wang, Y.; Shi, L.; Pang, W.; Zhu, Q.; Xu, G.; Lu, F., Propeller-Like Multicomponent Microstructures: Self-Assemblies of Nanoparticles of Poly(vinyl alcohol)-Coated Ag and/or Cu_2O. *J. Phys. Chem. B* **2006,** *110*, 14702-14708.
3. Yin, M.; Wu, C.-K.; Lou, Y.; Burda, C.; Koberstein, J. T.; Zhu, Y.; O'Brien, S., Copper Oxide Nanocrystals. *J. Am. Chem. Soc.* **2005,** *127*, 9506-9511.
4. Wang, M.; Sun, L.; Lin, Z.; Cai, J.; Xie, K.; Lin, C., p-n Heterojunction Photoelectrodes Composed of Cu_2O-Loaded TiO_2 Nanotube Arrays with Enhanced Photoelectrochemical and Photoelectrocatalytic Activities. *Energy Environ. Sci.* **2013,** *6*, 1211-1220.
5. Ai, Z.; Zhang, L.; Lee, S.; Ho, W., Interfacial Hydrothermal Synthesis of Cu@Cu_2O Core-Shell Microspheres with Enhanced Visible-Light-Driven Photocatalytic Activity. *J. Phys. Chem. C* **2009,** *113*, 20896-20902.
6. Zhang, Z.; Wang, P., Highly Stable Copper Oxide Composite as an Effective Photocathode for Water Splitting via a Facile Electrochemical Synthesis Strategy. *J. Mater. Chem.* **2012,** *22*, 2456-2464.
7. Wei, L.; Shifu, C., Preparation and Characterization of p-n Heterojunction Photocatalyst Cu_2O / In_2O_3 and its Photocatalytic Activity under Visible and UV Light Irradiation. *J. Electrochem. Soc.* **2010,** *157*, H1029-H1035.
8. Tahir, D.; Tougaard, S., Electronic and Optical Properties of Cu, CuO and Cu_2O Studied by Electron Spectroscopy. *J. Phys. Condens. Matter* **2012,** *24*, 175002.